A&A 394, 873–882 (2002)
DOI: 10.1051/0004-6361:20021335

Astronomy & Astrophysics

Hot dust in normal star-forming galaxies: $JHKL'$ photometry of the ISO Key Project sample⋆

L. K. Hunt[1], C. Giovanardi[2], and G. Helou[3]

[1] Istituto di Radioastronomia-Firenze/CNR, Largo E. Fermi 5, 50125 Firenze, Italy
[2] INAF-Osservatorio Astrofisico di Arcetri, Largo E. Fermi 5, 50125 Firenze, Italy
e-mail: giova@arcetri.astro.it
[3] IPAC-Caltech, Pasadena, CA, USA
e-mail: gxh@ipac.caltech.edu

Received 13 August 2002 / Accepted 12 September 2002

Abstract. We present JHK and 3.8 μm (L') photometry of 26 galaxies in the *Infrared Space Observatory* (ISO) Normal Galaxy Key Project (KP) sample and of seven normal ellipticals with the aim of investigating the origin of the 4 μm emission. The majority of the KP galaxies, and all the ellipticals, have $K - L \lesssim 1.0$, consistent with stellar photospheres plus moderate dust extinction. Ten of the 26 KP galaxies have $K - L \gtrsim 1.0$, corresponding to a flat or rising 4 μm continuum, consistent with significant emission from hot dust at 600–1000 K. $K - L$ is anticorrelated with ISO flux ratio $F_{6.75}/F_{15}$, weakly correlated with line ratio [O I]/[C II], but not with [C II]/FIR or IRAS ratio F_{60}/F_{100}. Photodissociation-region models for these galaxies show that the hot dust responsible for red $K - L$ resides in regions of high pressure and intense far-ultraviolet radiation field. Taken together, these results suggest that star formation in normal star-forming galaxies can assume two basic forms: an "active", relatively rare, mode characterized by hot dust, suppressed Aromatic Features in Emission (AFEs), high pressure, and intense radiation field; and the more common "passive" mode that occurs under more quiescent physical conditions, *with* AFEs, and *without* hot dust. The occurrence of these modes appears to only weakly depend on the star-formation rate per unit area. Passive star formation over large scales makes up the bulk of star-forming activity locally, while the "active" regime may dominate at high redshifts.

Key words. galaxies: spiral – galaxies: starbursts – galaxies: ISM – ISM: dust

1. Introduction

The *Infrared Space Observatory* (ISO) mission has provided an unprecedented view of the interstellar medium (ISM) in galaxies from the near-infrared (NIR) continuum between 3 and 5 μm to the C^+ fine-structure transition at 158 μm and beyond. Infrared spectra (3 to 12 μm) obtained by ISO-PHOT reveal the mid-infrared (MIR) emission from *normal galaxies* to be characterized by the Aromatic Features in Emission (AFEs) at 3.3, 6.2, 7.7, 8.6, and 11.3 μm, and an underlying continuum which contributes about half the luminosity in the 3 to 12 μm range (Helou et al. 2000).

However, the ISO data have also raised many questions about the ISM constituents. In particular, the nature of the dust responsible for the AFEs is not yet clear, and the debate over three-dimensional Very Small Grains (VSGs), two-dimensional Polycyclic Aromatic Hydrocarbon molecules (PAHs), or Amorphous Hydrogenated Carbon particles (HACs), and their relative contribution in different environments is still underway (Jenniskens & Désert 1993; Lu 1998; Cesarsky et al. 1998). Moreover, the relationship between the carriers of the AFEs and the underlying continuum remains obscure (Boulanger et al. 1996; Helou et al. 2000).

A related question is the relative contributions of dust in the ISM, stellar photospheres, and circumstellar dust to the MIR radiation in spirals and ellipticals. IRAS data already convincingly showed that the MIR emission in spirals is mainly due to a continuum from small grains transiently heated to high temperatures and AFEs. On the other hand, in elliptical galaxies the ISM-to-stellar ratio is generally low, so that photospheric and circumstellar emission from evolved red giants may contribute significantly to the MIR (Knapp et al. 1992; Mazzei & de Zotti 1994). It has been argued, though, that the same IRAS color-color relation (e.g., Helou 1986) holds for ellipticals and spirals, which implies a similar ISM origin (Sauvage & Thuan 1994).

The continuum component between 3 and 5 μm can be extrapolated fairly well to the continuum level at 9–10 μm (Helou et al. 2000), which suggests that some of the 3–5 μm continuum must be produced by the ISM. Nevertheless, a portion of the 3–5 μm continuum must arise from stellar photospheres since

Send offprint requests to: L. K. Hunt,
e-mail: hunt@arcetri.astro.it
⋆ Based on data obtained at TIRGO, Gornergrat, Switzerland.

they dominate the emission at 1–2 μm. Although the signal-to-noise in the 3–5 μm ISO spectra is relatively low, that is the spectral region where the MIR spectra of the 43 galaxies observed by Helou et al. (2000) show the most significant galaxy-to-galaxy variation. To understand the physical origin of this, and assess the relationship of the MIR continuum to the ubiquitous AFEs, it is necessary to separate the ISM contribution from that of stellar photospheres and circumstellar dust. To this end, we have acquired $JHKL'$ photometry of the galaxies studied in Helou et al. (2000), which constitutes one of the ISO Normal Galaxy Key Projects. A variety of ISO observations have been secured for this sample, including mid-infrared spectra (Helou et al. 2000), ionic and atomic fine-structure line fluxes (Malhotra et al. 1997; Malhotra et al. 2001), mid-infrared maps at 7 and 15 μm, and a small number of 4.5 μm images (Dale et al. 2000).

The rest of the paper is organized as follows: Sect. 2 describes the observations, reduction, and photometric calibration. We compare the $JHKL$ colors of the sample galaxies with their ISO properties in Sect. 3, and with photodissociation-region models in Sect. 4. Section 5 discusses the nature of the 4 μm continuum, and our interpretation of these results in terms of "active" and "passive" star formation.

2. The sample, the observations, and the colors

The ISO Key Project for Normal Galaxies (PI: G. Helou, KP) was proposed to study the ISM of a broad range of normal galaxies using several instruments aboard ISO. The sample, described in Malhotra et al. (2001), is designed to capture the great diversity among galaxies, in terms of morphology, luminosity, far-infrared-to-blue luminosity ratio FIR/B, and IRAS colors. The project obtained ISO observations of 69 galaxies, including nine relatively nearby and extended objects. The remaining 60 galaxies cover the full range of observed morphologies, luminosities, and star-formation rates seen in normal galaxies, and includes five dwarf irregulars discussed in Hunter et al. (2001). Two of these, NGC 1156 and NGC 1569, are part of our observed sample, and are also the two nearest objects (6.4 and 0.9 Mpc, respectively). The median distance of the KP sample (including these nearby objects, and with $H_0 = 75\,\mathrm{km\,s^{-1}/Mpc}$) is 34 Mpc (Dale et al. 2000). This means that with the 14″ observing aperture we are sampling a central region roughly 1 kpc in radius. We observed 26 KP galaxies.

We also selected seven quiescent ellipticals from the sample of early-type galaxies observed with ISO by Malhotra et al. (2000), or with published JHK photometry (Frogel et al. 1978). Several of the latter do not have the rich array of ISO observations obtained for the KP galaxies.

2.1. Observations

The observations were acquired at the 1.5 m f/20 Infrared Telescope at Gornergrat (TIRGO[1]), with a single-element InSb detector. The photometer is equipped with standard broad-band filters (J 1.2 μm, H 1.6 μm, K 2.2 μm, and L' 3.8 μm) with diaphragms in the focal plane defining the aperture dimensions. The galaxy coordinates were taken from NED[2] and checked with the DSS[3]; all observations were acquired with a 14″ aperture, after maximizing the infrared signal. Sky subtraction was performed with a wobbling secondary at frequencies that ranged from 2.1 to 12.5 Hz, according to the integration time for the individual measurement. The modulation direction was in a EW direction, with an amplitude of roughly 3′. Beam switching was used to eliminate linear variations in sky emission.

Photometric calibration was achieved by similarly observing several standard stars nightly from the CIT (Elias et al. 1982) and the ARNICA (Hunt et al. 1998) standard lists. Nightly scatter of the photometric zero point was typically 5% or better in JHK and 8% or better in L'.

The final photometry for the 33 galaxies observed is reported, together with their basic data, in Table 1. In what follows, we have transformed $K{-}L'$ to $K-L$ (this last is centered at 3.5 μm) using the transformation by Bessell & Brett (1988), and we will use $K-L$ to denote such colors. In the various plots and when testing for correlations, the NIR data have also been corrected for *i)* Galactic extinction according to Schlegel et al. (1998) and Cardelli et al. (1989), and *ii)* K dimming using the precepts mentioned in Hunt & Giovanardi (1992).

2.2. JHKL colors

The NIR colors of the observed galaxies are shown in Fig. 1. The filled symbols represent those (10) galaxies with $K-L \gtrsim 1.0$, that is a rising continuum (see below). Also shown in the diagram are H II galaxies taken from Glass & Moorwood (1985) and starbursts from Hunt & Giovanardi (1992). Three low-metallicity blue compact dwarfs (BCDs) are also shown as asterisks: NGC 5253 (Glass & Moorwood 1985), II Zw 40 (Thuan 1983), but no J, and SBS 0335-052 (Hunt et al. 2001). The BCDs have the most extreme colors since they tend to be quite blue in $J-H$ (because of low metallicity and youth), and red in $K-L$ (because of ionized gas and hot dust).

Mixing curves show how the colors change when various physical processes increasingly contribute to the emission observed (see Hunt & Giovanardi 1992); they illustrate that, on the basis of NIR color, it is possible to distinguish among stellar photospheric emission, "passive" dust in extinction, and "active" dust in emission. $H-K$ tends to be red (>0.35) for both dust extinction and dust emission, while $K-L$ is red only because of emission by dust or ionized gas (see the free-free line). Thus red $K-L$ can be used to signal a substantial contribution from hot dust emission in the observing aperture. The 600 and 1000 K mixing curves span the observed colors quite well, and although the VSG emission is not thermalized, the

[1] The Infrared Telescope at Gornergrat (Switzerland) is operated by CAISMI-CNR, Arcetri, Firenze.

[2] The NASA/IPAC Extragalactic Database (NED) is operated by the Jet Propulsion Laboratory, California Institute of Technology, under contract with the U.S. National Aeronautics and Space Administration.

[3] The DSS was produced at the Space Telescope Science Institute under U.S. Government grant NAG W-2166.

Table 1. Basic data and NIR photometry

Name	R.A. (J2000)	Dec.	RH Type	m_B	V_H	Size	K	$J-H$	$H-K$	$K-L'$	Notes
	[h m s]	[^{o} ' "]		[mag]	[km s^{-1}]	[arcmin]	[mag]	[mag]	[mag]	[mag]	
(1)	(2)	(3)	(4)	(5)	(6)	(7)	(8)	(9)	(10)	(11)	(12)
NGC 0278	00 52 04.4	47 33 01	SAB(rs)b	11.5	641	2.1 x 2.0	10.11±0.02	0.71±0.03	0.24±0.03	0.47±0.10	
NGC 0520	01 24 35.0	03 47 37	S;P	12.4	2266	1.9 x 0.7	10.02 0.01	1.06 0.03	0.58 0.02	1.58 0.16	starburst
NGC 0695	01 51 14.3	22 34 56	S0?P	13.8	9735	0.8 x 0.7	12.14 0.03	0.98 0.06	0.66 0.05	1.44 0.12	HII
NGC 0777	02 00 14.8	31 25 48	E1	12.5	4985	2.5 x 2.0	9.68 0.02	0.93 0.06	0.28 0.05	0.34 0.15	
NGC 0821	02 08 21.2	10 59 42	E6?	11.7	1753	2.6 x 1.6	9.28 0.03	0.70 0.05	0.34 0.05	0.11 0.10	
UGC 02238	02 46 17.5	13 05 44	Im?	14.6	6436	1.4 x 1.3	10.63 0.02	1.22 0.06	0.64 0.05	0.74 0.14	LINER
NGC 1156	02 59 42.3	25 14 13	IB(s)m	12.3	375	3.3 x 2.5	12.70 0.03	0.72 0.04	0.24 0.04	2.49 0.11	
NGC 1222	03 08 56.9	-02 57 18	S0;P	13.6	2452	1.1 x 0.9	10.59 0.05	0.81 0.09	0.42 0.07	1.35 0.15	
UGC 02519	03 09 19.9	80 07 50	Scd?	14.3	2377	1.2 x 0.7	12.17 0.03	0.73 0.04	0.34 0.04	1.87 0.08	
NGC 1266	03 16 00.9	-02 25 40	(R')SB(rs)0;P	13.9	2194	1.5 x 1.0	10.85 0.04	0.93 0.06	0.33 0.06	1.70 0.12	LINER
UGC 02855	03 48 22.6	70 07 57	SABc	13.5	1202	4.4 x 2.0	11.05 0.02	0.77 0.05	0.54 0.04	0.86 0.18	
NGC 1569	04 30 49.5	64 50 54	IBm	11.9	-104	3.6 x 1.8	10.00 0.03	0.64 0.05	0.23 0.05	0.90 0.09	Sy1
NGC 1600	04 31 40.0	-05 05 10	E3	11.9	4718	2.5 x 1.7	9.79 0.03	0.72 0.06	0.29 0.06	0.20 0.10	
NGC 1700	04 56 56.3	-04 51 57	E4	12.2	3881	3.3 x 2.1	9.16 0.03	0.65 0.06	0.28 0.05	0.19 0.12	
NGC 2300	07 32 20.8	85 42 32	SA0^0	12.1	1922	2.8 x 2.0	9.18 0.02	0.65 0.05	0.36 0.05	0.28 0.07	
NGC 2388	07 28 53.6	33 49 08	S?	14.7	4134	1.0 x 0.6	10.17 0.01	0.91 0.02	0.49 0.01	0.78 0.05	HII
NGC 3583	11 14 10.8	48 19 04	SB(s)b	11.9	2136	2.8 x 1.8	10.06 0.02	0.78 0.03	0.34 0.03	0.53 0.06	
NGC 3665	11 24 43.5	38 45 45	SA(s)0^0	11.8	2080	2.5 x 2.0	9.31 0.03	0.80 0.16	0.18 0.12	0.54 0.07	
NGC 3683	11 27 31.8	56 52 39	SB(s)c?	13.2	1716	1.9 x 0.7	9.94 0.01	0.86 0.02	0.37 0.01	0.53 0.06	
NGC 3705	11 30 07.5	09 16 37	SAB(r)ab	11.9	1018	4.9 x 2.0	9.97 0.05	0.81 0.05	0.15 0.06	0.34 0.08	
NGC 3949	11 53 41.4	47 51 32	SA(s)bc	11.5	807	2.9 x 1.7	10.68 0.01	0.69 0.02	0.21 0.01	0.55 0.09	
NGC 4102	12 06 23.1	52 42 40	SAB(s)b?	12.0	837	3.0 x 1.7	8.69 0.01	0.88 0.02	0.42 0.01	0.57 0.03	LINER
NGC 4194	12 14 09.6	54 31 35	IBm;P	13.0	2506	1.8 x 1.1	10.07 0.02	0.76 0.03	0.45 0.03	1.15 0.05	HII
NGC 4490	12 30 36.0	41 38 41	SB(s)d;P	10.2	565	6.3 x 3.1	11.02 0.01	0.63 0.02	0.21 0.01	0.64 0.10	
NGC 4519	12 33 30.3	08 39 16	SB(rs)d	12.3	1220	3.2 x 2.5	12.06 0.04	0.79 0.17	0.82 0.12	1.66 0.12	
NGC 5433	14 02 36.1	32 30 36	Sdm	14.1	4354	1.6 x 0.4	10.81 0.01	0.84 0.07	0.23 0.02	1.40 0.27	
NGC 5713	14 40 11.5	00 17 30	SAB(rs)bc;P	12.2	1883	2.8 x 2.5	10.51 0.05	0.98 0.04	0.24 0.06	0.67 0.09	
NGC 5866	15 06 29.5	55 45 47	S0$_3$	10.7	672	4.7 x 1.9	8.90 0.01	0.85 0.02	0.36 0.01	0.42 0.03	HII/LINER
NGC 5962	15 36 31.8	16 36 28	SA(r)c	12.0	1958	3.0 x 2.1	10.10 0.10	0.72 0.10	0.25 0.10	0.26 0.10	
NGC 6286	16 58 31.7	58 56 14	Sb;P	14.1	5501	1.3 x 1.2	10.85 0.05	0.96 0.05	0.56 0.06	1.04 0.09	LINER
NGC 7626	23 20 42.4	08 13 02	E;P	12.2	3403	2.6 x 2.3	9.73 0.05	0.72 0.09	0.35 0.09	0.60 0.12	
IR 23365+3604	23 39 01.3	36 21 09	S?Ba?;P	16.3	19336	0.5 x 0.3	12.57 0.06	1.29 0.10	0.52 0.10	2.86 0.15	LINER
MRK 0331	23 51 26.9	20 35 08	S?	14.9	5541	0.7 x 0.4	10.25 0.15	0.79 0.15	0.44 0.15	1.45 0.10	HII, Sy2

Basic data are from NED. The errors reported for the NIR photometry (columns 8 through 11) are 1σ.

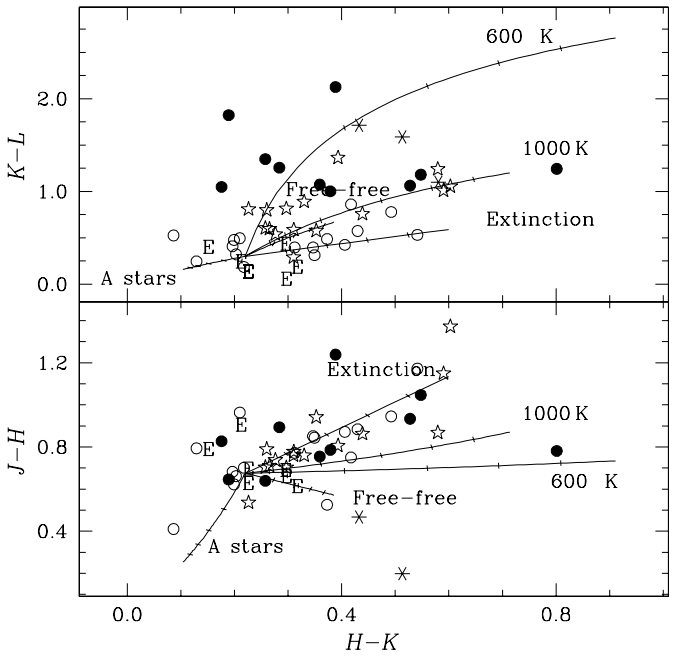

Fig. 1. NIR color-color diagram; the $K - L$ color in the top panel is transformed from $K - L'$ as described in the text. Filled symbols refer to galaxies with $K - L > 1.0$. The 7 quiescent ellipticals are indicated with an E. Shown as stars are H II galaxies taken from Glass & Moorwood (1985) and starbursts from Hunt & Giovanardi (1992), and shown as asterisks the BCDs (see text). Mixing curves show how the colors change when various physical processes increasingly contribute to the emission observed (see Hunt & Giovanardi 1992); the end points of the mixing curves indicate equal K-band contributions from stars and the process (hot dust, ionized gas, A stars). The tick marks on the extinction line show unit A_V magnitude increments.

curves show that the NIR colors are consistent with dust at these temperatures.

The $K - L$ color can also provide an estimate of the slope of the spectral energy distribution (SED) between 2 and 4 μm. Using the zero-magnitude fluxes given in Koornneef (1983), and assuming a power-law dependence $f_\nu \propto \nu^\alpha$, we find that $K - L = -0.50\,\alpha + 0.95$. Therefore[4], $K - L \gtrsim 1.0$ is where the slope α changes sign and becomes negative, signifying a continuum f_ν rising with increasing wavelength; when $K - L < 1.0$, α is positive. The mean α averaged over the entire KP sample is > 0, with $f_\nu \propto \nu^{+0.65}$ (Helou et al. 2000). If we include the ellipticals, the median $K - L$ of our 33 galaxies is 0.50, which gives $\alpha = 0.90$, steeper than, but consistent with, Helou et al. (2000). If only the ISO Key Project galaxies are considered, median $K - L = 0.68$, corresponding to $\alpha = 0.54$, remarkably close to that reported in Helou et al. The median $K-L$ for the ellipticals only is 0.21, which corresponds to a very steep falling continuum with $\alpha = 1.5$.

The mixing curves shown in Fig. 1 illustrate what fraction of the observed flux is due to hot dust; they assume a mix of stellar photospheres with intrinsic stellar color $(K - L)_* = 0.3$, or $(K - L')_* = 0.5$, plus dust emission. When the SED is flat at 4 μm ($K - L \approx 1.0$, slope $\alpha = 0$), 600 K hot dust comprises roughly 5% of the total K-band flux; hotter dust (e.g., 1000 K) would constitute 30%. It is unlikely that flat or rising continua are due to free-free emission from ionized gas, since even with a 50% emission fraction from gas, the continuum is still falling [$(K - L) = 0.7$]. This means that $K - L$, or alternatively the slope of the 4 μm continuum, is a remarkably sensitive diagnostic of hot dust: small K-band fractions (5–30%) of dust emission cause large variations (0.6 mag) in the $K - L$ color. A 50/50 K-band mix of hot dust and stars would produce a $K - L$ color between 1.2 and 2.7, depending on the dust temperature; NGC 4519, the galaxy with the reddest $H - K$ (= 0.82), may contain such a mix.

[4] The intercept climbs from 0.95 to 1.10 if we adopt instead the scale of Wilson et al. (1972).

3. Comparison with ISO photometry and spectra

If the non-stellar 3.8 μm flux is truly associated with hot dust, we would expect to find correlations between ISO MIR observations and L', if both arise from a similar small-grain population. Also, observations of the two most important photo-dissociation region (PDR) cooling lines, [C II] and [O I], suggest that gas and dust temperatures increase together (Malhotra et al. 2001); we might therefore expect trends with these line fluxes and ratios and $K - L$.

3.1. Broadband fluxes

We first checked that our ground-based (small-aperture) L' fluxes were broadly consistent with the ISO fluxes at $F_{6.75}$ and F_{15} (Dale et al. 2000). All three are mutually correlated (not shown), except for two cases (NGC 278 and NGC 5713) where the ISO flux is substantially larger than expected from the general trend. This discrepancy is almost certainly due to aperture effects, since the ground-based data are acquired in a 14″ aperture, while the ISO values published in Dale et al. (2000) are total fluxes as extrapolated from curves of growth. NGC 1569 is generally an outlier; however, its properties are similar to those of other low-metallicity dwarf irregulars (see Hunter et al. 2001). The other dwarf irregular in our observed sample is NGC 1156, again a clear outlier in most of the subsequent plots and correlations. As noted in Sect. 2, these galaxies are also the two closest galaxies, which considerably complicates the comparison of the ISO and our ground-based 14″ aperture data.

We next compare ISO colors with $K - L$ in Fig. 2 where $F_{6.75}/F_{15}$ and the "hybrid" color $F_{3.8}/F_{15}$ are plotted against $K - L$. Ground-based $K - L$ turns out to be correlated ($2.5\,\sigma$) with $F_{6.75}/F_{15}$[5], but is uncorrelated with the hybrid color. The sense of the $F_{6.75}/F_{15}$ vs. $K - L$ correlation is such that *redder* $K - L$ implies *lower* $F_{6.75}/F_{15}$. NGC 1569 stands out since it has a very low $F_{6.75}/F_{15}$ ratio for its $K-L$ color. As an extreme case, in Fig. 2, we have also plotted SBS 0335-052 (not considered in the correlation), using the ISO data from Thuan et al. (1999) and $K - L$ from Hunt et al. (2001). SBS 0335-052 is an

[5] If the nearest objects, NGC 1569 and NGC 1156, are eliminated from the regression the significance becomes $4.0\,\sigma$. If, in addition, the reddest $K-L$ value (IRAS 23365+3604) is eliminated, the significance becomes $2.1\,\sigma$.

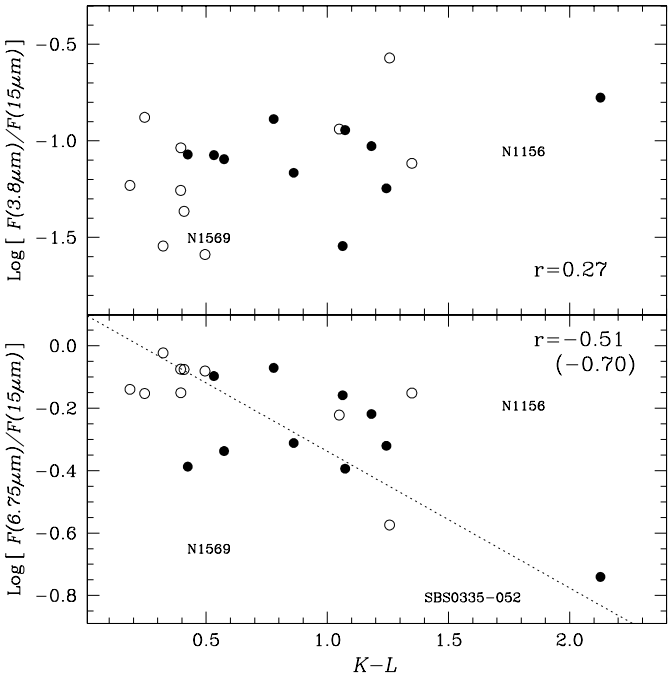

Fig. 2. Hybrid ground-based/ISO color-color plot: the top panel shows the ratio of the 3.8 μm flux (not transformed to L) and F_{15} plotted against $K-L$, and the bottom panel the ratio of $F_{6.75}$ and F_{15} plotted against $K-L$. The dotted line shows the best-fit regression; the correlation coefficients are shown in each panel (parentheses denote the coefficient without the two nearest galaxies NGC 1569 and NGC 1156). Solid dots are used when the corrected $H-K>0.35$.

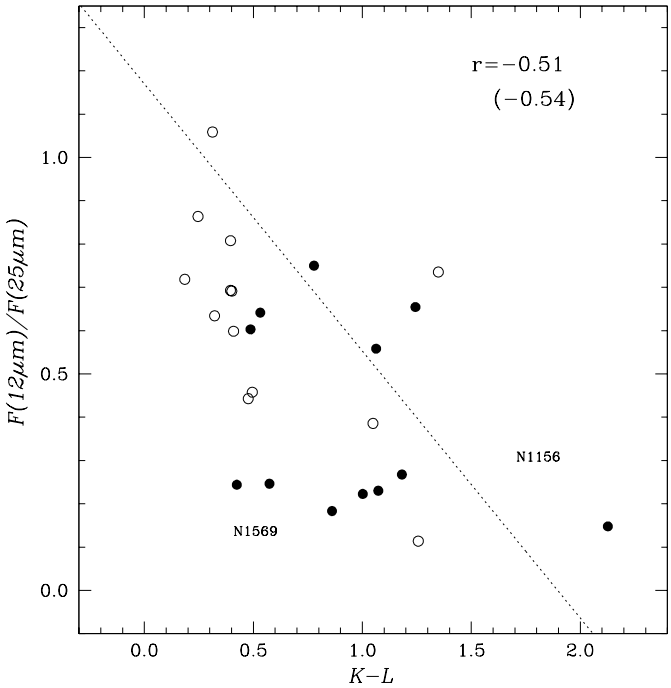

Fig. 3. IRAS 12 μm/25 μm flux ratio vs. $K-L$. No IRAS upper limits are shown. Solid points refer to galaxies with a corrected $H-K>0.35$. The best-fit regression is shown together with the correlation coefficient (in parentheses is that without NGC 1156 and NGC 1569, the two nearest galaxies).

unusual BCD with 1/40 solar metallicity, and the ISO spectrum shows no AFEs; not surprisingly Fig. 2 shows that this galaxy has a lower $F_{6.75}/F_{15}$ ratio than any of the galaxies in the ISO sample.

Since dust temperatures in large "classical" grains are connected with the IRAS flux ratio F_{60}/F_{100}, and since this ratio and $F_{6.75}/F_{15}$ are anticorrelated (Dale et al. 2000), we might expect $K-L$ to also be anticorrelated with F_{60}/F_{100}. We found no such correlation but note, instead, that IRAS F_{12}/F_{25} is anticorrelated ($2.6\,\sigma$) with $K-L$[6], as shown in Fig. 3[7]. Together with the trend with $K-L$ and $F_{6.75}/F_{15}$, this means that the presence of hot dust is: *a)* usually linked to the suppression of AFEs which dominate the 12 μm band (Helou et al. 1991), and *b)* largely independent of the temperature and characteristics of the large grains.

3.2. Line measurements

In PDRs and H II regions, gas and dust are intimately related. In ionized regions, gas and dust compete for far-ultraviolet (FUV) photons, but the neutral gas in PDRs is heated predominantly by photoelectrons from small dust grains (Watson 1972; Hollenbach & Tielens 1997). Neutral gas is cooled primarily by atomic and ionic fine-structure lines, [C II] (158 μm) and [O I] (63 μm), and these lines can be used as diagnostics for the physical conditions in the PDR gas (Tielens & Hollenbach 1985): the [O I] line is expected to become more important relative to [C II] in warmer and denser gas. [C II] and [O I] line fluxes for the galaxies in our sample have been measured by ISO (Malhotra et al. 2001), and in this section we analyze those measurements in the context of our new photometry.

An important diagnostic is the ratio of [C II] and the far-infrared flux (FIR), since it measures essentially the efficiency of the photoelectric heating of the gas by dust grain ejection. This ratio [C II]/FIR tends to decrease with warmer FIR colors F_{60}/F_{100} and increasing star-formation activity as indicated by FIR/B (Malhotra et al. 2001). Moreover, warmer gas, as signified by smaller [C II]/[O I], correlates with warm dust or larger F_{60}/F_{100}; this last is the most significant correlation in the study by Malhotra et al. (2001). Since red $K-L$ should be related to hot dust and its temperature, we might expect to find similar correlations with normalized FIR line fluxes and ratios. However, this supposition is not borne out by the data (see Fig. 4): we find no correlation between $K-L$ and [C II]/FIR, and only a weak anticorrelation between $K-L$ and [C II]/[O I]. Again, $K-L$ appears to be measuring a hot-dust phase, not closely connected to the properties of the cooler dust.

4. PDR models

Photodissociation models for all the galaxies in our sample have been reported in Malhotra et al. (2001), calculated from

[6] If the object with the reddest $K-L$ (IRAS 23365+3604) is eliminated from the regression, the significance becomes 2.4 σ.

[7] Although these galaxies were selected to be sufficiently distant, given the size of the IRAS beams compared to our ground-based photometry, aperture effects almost certainly contribute significantly to the scatter.

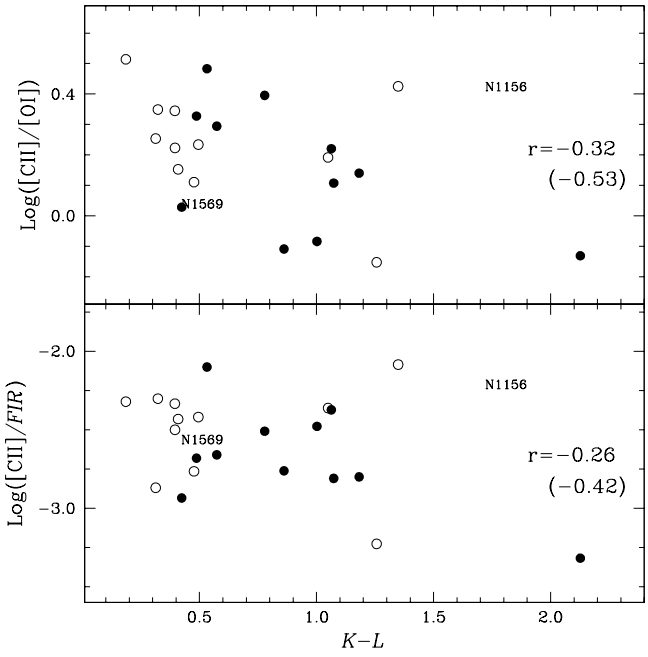

Fig. 4. ISO emission-line ratios vs. $K-L$. The top panel shows the log of the ratio of [C II] (158 μm) and [O I] (63 μm) line fluxes vs. $K-L$, and the bottom panel the log of the ratio of [C II] and FIR vs. $K-L$. The correlation coefficients are shown in each panel (the correlation coefficient in parentheses is that without NGC 1156 and NGC 1569, the two nearest objects). Solid dots refer to galaxies with corrected $H-K>0.35$.

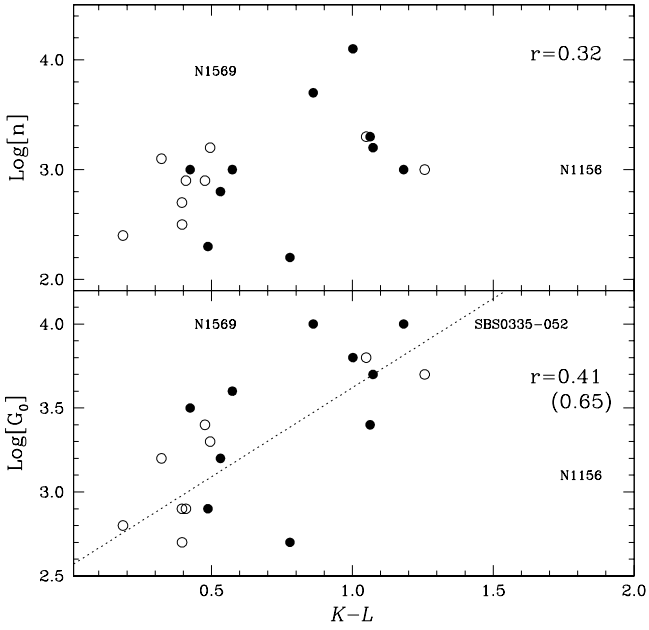

Fig. 5. Log n (upper panel) and Log G_0 (lower) plotted against $K-L$. The PDR parameters are taken from Malhotra et al. (2001). The dotted line in the lower panel shows the best-fit regression; the correlation coefficients are shown in each panel. Solid points refer to galaxies with corrected $H-K>0.35$. Estimate of correlation coefficients and regression include all objects (the parentheses contain the coefficient without NGC 1156 and NGC 1569, the two nearest galaxies).

the model grids of Kaufman et al. (1999). These models calculate the line emission in [C II] and in [O I] (including the line at 145 μm) and the dust continuum emission for a plane slab of gas illuminated on one side by FUV radiation. Gas heating in the models is dominated by photoelectrons ejected from classical (large) grains and from VSGs according to the recipe of Bakes & Tielens (1994). From these models, it is possible to infer values for the neutral gas density n and the FUV radiation field G_0, as well as for the pressure P and temperature T of the gas.

Figure 5 shows gas density n and FUV flux G_0, as derived from PDR models, plotted against $K-L$. Without NGC 1156 (one of the two nearest galaxies), $K-L$ is well correlated with G_0, at the $3.5\,\sigma$ level. This is a clear indication that red $K-L$ is connected to strong FUV radiation fields. Also shown in Fig. 5 is SBS 0335-052, with a $G_0 \sim 10\,000$ times stronger than the local value (Dale et al. 2001); this galaxy follows the same correlation.

We then examine whether the primary dependency of red $K-L$ color is on neutral gas temperature T or on its pressure P, given that the $K-L$ color is independent, or roughly so, of neutral gas density n. The relevant PDR parameters are plotted in Fig. 6 where T and P as inferred from the PDR models are plotted versus $K-L$. The thermal pressure P of the PDR is expected to be approximately equal to the thermal pressure of the adjacent H II region (Malhotra et al. 2001). The correlation between P and $K-L$ is weak but becomes significant (2.8σ) once we exclude NGC 1156. There is no apparent correlation between T and $K-L$. Taken together, these results suggest that the PDR pressure (roughly equal to the H II pressure) and the FUV radiation field G_0 are the main factors which govern the existence of hot dust in star-forming galaxies; neutral gas density and temperature by themselves are less important influences.

5. The nature of the 4 μm continuum

We first discuss the nature of the 4 μm continuum, as inferred from our observations. Because of the filter cutoff, L' misses the 3.3 μm aromatic emission feature (e.g., Moorwood & Salinari 1983; Moorwood 1986), and thus should be a measure of the AFE-free continuum. As mentioned in Sect. 2.2, the $K-L$ color is a sensitive diagnostic of the fraction of hot dust contained in the observing aperture. The 4 μm continuum of most of the galaxies we observed is consistent with stellar photospheres together with moderate dust extinction. As expected, the best cases for pure stellar $K-L$ colors are the ellipticals which have median $K-L=0.21$. Within the 14″ observing aperture, we find no evidence for circumstellar dust in the ellipticals, since their NIR colors are inconsistent with dust emission at any temperature.

In roughly a third of our sample, the $K-L$ color ($\gtrsim$1) signifies a flat or rising 4 μm continuum. Even a small fraction (5%) of hot (600 K) dust can cause this inflection, and is very likely the cause of the large variance in the 3–5 μm continua, as noted by Helou et al. (2000). Because of the characteristics of the L' filter, we conclude that the red $K-L$ color must represent a continuum property, rather than short-wavelength AFEs. Such a continuum is typically accompanied by a lower

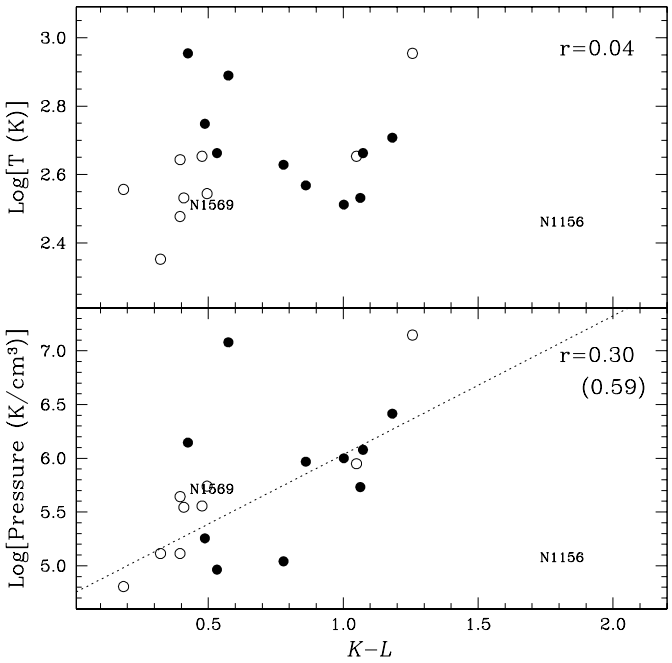

Fig. 6. Log T (upper panel) and Log P (lower) plotted against $K-L$. The PDR parameters are taken from Malhotra et al. (2001). The dotted lines show the best-fit regression; the correlation coefficients are reported in each panel. Solid points refer to galaxies with corrected $H-K>0.35$. Estimates of regression line and correlation coefficients include all galaxies (the parentheses contain the coefficient without the two nearest objects, NGC 1156 and NGC 1569).

$F_{6.75}/F_{15}$ ratio (see Fig. 2), due either to AFE suppression or to an F_{15} excess (or both). Either way, we are observing a significant fraction of hot dust in the central regions of these galaxies, with physical conditions that favor red $K-L$, namely strong G_0 and high pressure.

5.1. Physical conditions in star forming regions with hot dust

Malhotra et al. (2001) describe a physical picture in which the infrared line emission arises in a PDR which surrounds an expanding H II region. They suggest that the ISO diagnostics are probing the typical distance from an OB star or cluster to the PDR gas, rather than the global rate of star formation. Our new 4 μm data are consistent with this picture. Red $K-L$ tends to be associated with an intense UV radiation field G_0. The trend shown in Fig. 5 suggests that rising 4 μm continua are observed when UV radiation field $G_0 \gtrsim 10^{3.5}$. It is easy to show that such an intense G_0 must be found within a few tens of pc from the ionizing star cluster. Assuming the FUV luminosity of a single star to be 10^{39} erg s^{-1} (!), and with a star cluster consisting of 100 OB stars, the typical distance for $G_0 = 10^{3.5}$ is 10 pc. In the same conditions, at a distance of 100 pc we would need 10 000 massive stars, more than all but those in the most luminous Super Star Clusters (SSCs: e.g., Calzetti et al. 1997; Turner et al. 2000). With the lower FUV luminosity from lower-mass stars, the distance to maintain the intense G_0 would be even smaller. Hence, it is likely that red $K-L$ is probing a region within a few tens of pcs from star clusters containing a few hundred OB stars. Such sizes are more than a hundred times smaller than the projected size of our observing aperture at the median distance of the sample (see Sect. 2).

Hot dust as measured by high-resolution 10–12 μm images of infrared-luminous starbursts also tends to be compact, and compact nuclear starbursts generally dominate their starburst activity (Soifer et al. 2001). Typical MIR sizes in the Soifer et al. sample range from <125 pc to ~1 kpc; however these may be partly overestimated since the spatial resolution for the nearest galaxy in their study (NGC 3690) is 210 pc arcsec^{-1} which procured mostly upper limits (<125 pc) for the size of the emitting regions.

The hot dust that gives rise to red $K-L$ must be heated by massive stars, and according to the PDR models, tends to be found in high-pressure environments and, from the above discussion, in close proximity of the H II region. This intense environment suppresses AFE emission, probably because of the strong UV radiation field, as proposed by earlier work (e.g., Normand et al. 1995). In the framework of an expanding H II region surrounded by a PDR, such conditions are likely to obtain in young H II regions, still embedded within their natal molecular cloud, which have not yet had time to break through the cloud surface. At first glance then, $K-L$ appears to be a measure of age: hot dust is found preferentially in young H II regions.

Nevertheless, the attribution of the rising 4 μm continuum to youth has some problems. Some very young systems have "normal" photospheric+extinction $K-L$ colors: the two brightest star clusters in NGC 1569 contain Wolf-Rayet (W-R) stars and their age has been estimated at <5 Myr (Origlia et al. 2001). We measure for NGC 1569 $K-L=0.7$, consistent with stellar photospheres + extinction, not with hot dust. Haro 2 (not in this sample) also contains W-R stars (Vacca & Conti 1992), and as such must be younger than 5 Myr, but $K-L=0.5$ (Thuan 1983). Thus, young systems are not necessarily associated with red $K-L$ and hot dust.

It also might be that $K-L$ is a diluted version of the flux ratio FIR/B, since variations in FIR/B, or star-formation activity, might be translated into variations of the hot-dust versus stellar fraction in our observing aperture. We investigate this in the top panel of Fig. 7, where we have plotted Log(FIR/B) vs. $K-L$. There is no correlation between these two quantities, although the galaxy with the highest value of FIR/B is associated with the reddest $K-L$ (IRAS 23365+3604). It is thus difficult to interpret $K-L$ as an indicator of generic star formation, since the hot dust traced by $K-L$ appears to be independent of the cooler grains traced by FIR.

5.2. "Active" and "passive" star formation

We therefore propose an alternative explanation, namely two "extreme" distinct modes of star formation. Recent models have shown that dust heating and molecular hydrogen production are more efficient in dense ($\gtrsim$500 cm^{-3}), compact ($\lesssim$100 pc) environments (Hirashita et al. 2002). Moreover, in low-metallicity BCDs, the size of the brightest star-forming

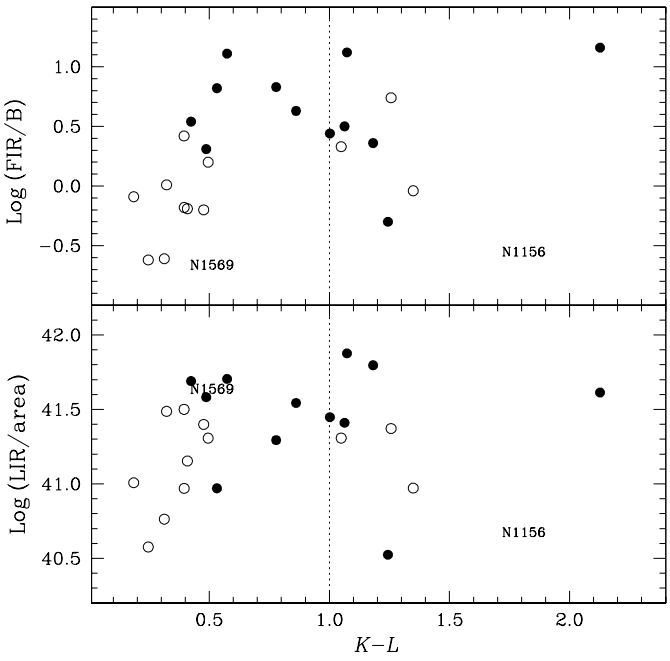

Fig. 7. Top panel: Log of the far-infrared-to-blue flux ratio FIR/B vs. $K-L$. FIR/B was taken from Dale et al. (2000), with FIR calculated according to the canonical dependence on F_{60} and F_{100} (Lonsdale Persson & Helou 1987). Bottom panel: Log $L_{\rm FIR}$/area versus $K-L$. $L_{\rm FIR}$ is the far-infrared luminosity and the area is the one of the ellipse with axes of the size reported in NED; $L_{\rm FIR}$/area is in erg s^{-1} kpc^{-2}. Galaxies with corrected $H-K \leq 0.35$ are shown as open circles, and $H-K > 0.35$ as filled ones. The vertical dotted line separates the "active" and "passive" regimes ($K-L \gtrsim 1$).

complex and its ionized gas density are very well correlated, with the densest regions being also the most compact (Hunt et al. 2002). In this same BCD sample, size and density are independent of age, since ages derived from recombination line equivalent widths are all $\lesssim$5 Myr. The correlations in the KP sample studied here seem to suggest a similar "dichotomy" since a strong UV radiation field, compact size, and pressure are associated with hot dust. The most compact dense regions in the BCD study by Hunt et al. (2002) were interpreted by them as indicative of "active" star formation, characterized by an intense physical environment harboring several hundreds/thousands of massive stars, and capable of efficiently heating dust. At a comparable star-formation rate, the less dense, less compact H II regions, termed "passive" by Hunt et al. (2002), are not able to heat dust efficiently because of the more diluted radiation field (Hirashita et al. 2002). We would argue that a rising 4 μm continuum is yet another signature of "active" star formation. A falling 4 μm continuum would be a sign of "passive" star formation, since the physical conditions are not able to produce a measurable fraction ($\gtrsim$5%) of hot dust; these more diffuse regions tend to have lower pressures, a less intense radiation field, and prominent AFEs in the MIR spectrum.

It might be argued that the two extremes are simply a measure of the star-formation rate (SFR). We have attempted to test this hypothesis by plotting the far-infrared luminosity per unit area $L_{\rm FIR}$/area against $K-L$, since $L_{\rm FIR}$ is frequently used to measure SFRs (e.g., Thronson & Telesco 1986). The bottom panel of Fig. 7 shows that the two quantities are not significantly correlated, nor is $K-L$ correlated with $L_{\rm FIR}$, that is without normalizing by the area (not shown). We already said that, although aperture effects may be important because of the large IRAS apertures, the top panel of the same figure shows no correlation between $K-L$ and the $L_{\rm FIR}$ *normalized* to the B band, nor with F_{60}/F_{100} (Sect. 3.1), yet another star formation indicator of common use. It appears, therefore, that the difference between the two extremes is of qualitative rather than quantitative origin.

It should be emphasized that "active" and "passive" star formation as we are defining them are *local* concepts: in a single galaxy, different regions may be characterized by either mode. In our Galaxy AFEs are notably diminished in H II regions (Cesarsky et al. 1998), and the MIR continuum tends to be stronger in denser structures (Abergel et al. 2002). M 82 is an another example, since where the infrared continuum peaks, there are few if any AFEs, but at the H II region-molecular cloud interface, the AFEs dominate (Normand et al. 1995). On galactic scales, there is also evidence that AFEs are diminished as the intensity of star formation increases (Förster Schreiber et al. 2002). With our ground-based data, we are investigating the properties of the dominant mode of star formation in the observing aperture, weighted by the brightness of the components. At longer wavelengths, higher spatial resolution is necessary to separate the two modes because in large apertures (e.g., IRAS, ISO), the cooler "standard" ISM virtually overwhelms any hot dust emission.

We further note that the bulk of star formation associated with starbursts is not necessarily of the "active" type. AFEs are always detected in galaxy nuclei with H II-region spectra (Roche et al. 1991); indeed these features dominate the integrated spectra of prototypical starbursts such as M 82 and NGC 253 (Sturm et al. 2000). They are also used to distinguish star formation from nuclear activity as the mechanism powering ultra-luminous infrared galaxies (ULIRGs, Genzel et al. 1998). This apparent "paradox" can be understood through the association of AFEs with the cool dust phase of the PDR (Haas et al. 2002). The hot dust we measure with $K-L$ is heated by the intense G_0 close to the H II region, and without high-resolution ($\lesssim$100 pc) measurements, the copious emission from the diffuse cooler dust and AFEs in the PDRs dominates the observed flux.

We have found evidence for hot dust in roughly 1/3 of the KP galaxies observed. It is not clear, however, whether the properties of these "active" star-forming galaxies are "extreme" compared to other examples of nuclear starbursts. An upper limit to the bolometric surface brightness of these objects can be deduced from the estimates given in Sect. 5.1: if we have a nuclear star cluster containing 100–1000 massive stars concentrated in a region of 10–100 pc in diameter, the bolometric surface brightness would be roughly $\lesssim 10^{11}$–$10^{12}\,L_\odot$ kpc^{-2}. This coincides approximately with the maximum mean surface brightness in the sample of low- and high-redshift starbursts of (Meurer et al. 1997). However, our estimate refers to the *nuclear star clusters*, not to the mean surface brightness over the observing aperture as in Meurer et al. As star clusters go, those

we have detected with $K - L$ are not extraordinary, since they are several times less bright than the resolved UV clusters described by Meurer et al. (1995).

What we have called the "active" mode is characterized by the formation of compact star-forming complexes within a high-pressure environment in an intense G_0. High pressure is also implicated in the strong galactic winds common in starbursts (Heckman et al. 1990). Such conditions also favor the formation of dusty SSCs (Bekki & Couch 2001), which are frequently found in merging galaxies (e.g., the Antennae: Whitmore et al. 1995; NGC 1741: Johnson et al. 1999), ULIRGs (Scoville et al. 2000; Shioya et al. 2001), and nuclear starbursts (e.g., M 82: Gallagher & Smith 1999; NGC 253: Keto et al. 1999; NGC 4214: Leitherer et al. 1996). Although somewhat uncertain, the nuclear star clusters inferred from our data have properties similar to SSCs, which could be yet another signature of "active" star formation.

5.3. Speculations for high-redshift studies

The physical environment of the "active" mode, especially high pressure, results naturally from interactions or mergers (Bekki & Couch 2001). Interestingly, interactions and mergers also produce red $K - L$ (Joseph et al. 1984). According to the Cold Dark Matter hierarchical clustering scenario of galaxy formation, the frequency and intensity of interactions are expected to increase with redshift, and semi-analytic recipes for galaxy formation based on "collisional starbursts" are successful at reproducing SFRs, colors, morphology, and mass trends with redshift (Somerville et al. 2001). Presently, the bulk of star formation in galaxies, including starburst galaxies and ULIRGs, takes place in the "passive" regime. But, due to the higher probability of strong tidal stresses and mergers, this situation may have been reversed in the past with the "active" regime being the preferred way to form stars at high redshift.

In this context, it is puzzling that we maintain that ULIRGs host passive star formation, although most if not all of them are mergers. The most plausible explanation of this paradox involves spatial resolution and the relative dominance of the "passive" ISM in ULIRGs (see Sect. 5.2). Given the large contribution from their cool ISM, the emission in ULIRGs integrated over large spatial scales appears passive. Even though "active" star formation must be occurring, it can be revealed only on small spatial scales, or by its hot dust. A case in point is the ULIRG in our sample, IRAS 23365+3604. This galaxy hosts several young ($\leq$10 Myr) star clusters (Surace et al. 2000), but is classified optically as a LINER (Veilleux et al. 1995). The LINER classification is probably not caused by an AGN, but rather by shocks generated in galactic superwinds (Lutz et al. 1999). We classify this object as "active" because of its extremely red $K - L$[8], but its ISO spectrum contains prominent AFEs (Tran et al. 2001). Young star clusters probably heat the dust responsible for the red $K - L$, while the ISO aperture encompasses the entire galactic disk (see Surace et al. 2000). Hence, IRAS 23365+3604 appears both active and passive: active because of its red $K - L$, and passive because of the overwhelming disk ISM.

Including the effects of active star formation in models of galaxy evolution (e.g., Granato et al. 2000) would not be straightforward. Nevertheless, when star formation occurs on spatial scales $\lesssim$100 pc (see Sect. 5.1), the intense radiation field, high pressure, and diminished AFEs should be taken into account. Indeed, suppressed AFEs coupled with the hot dust revealed by our photometry substantially alter the infrared spectrum of star-forming galaxies. This may be especially important in hierarchical merger models because of the supposed link between "active" star formation and interactions.

6. Conclusions

With our $JHKL'$ photometry, we have analyzed the 4 μm continuum and its relation with the MIR spectrum and FIR emission lines. We find the following:

1. The majority of the 26 KP galaxies have a falling 4 μm continuum, $K - L < 1.0$, consistent with stellar photospheres and moderate dust extinction. 10 of them have a flat or rising 4 μm continuum, $K - L \gtrsim 1.0$, consistent with a measurable fraction of 600–1000 K hot dust.
2. $K - L$ is anticorrelated with ISO ratios $F_{6.75}/F_{15}$ and IRAS ratio F_{12}/F_{25}, but only weakly with [C II]/[O I], and not at all with [C II]/FIR/ or IRAS ratio F_{60}/F_{100}.
3. PDR models for these galaxies show that the hot dust measured by red $K - L$ is associated with high pressures and intense far-ultraviolet radiation fields in compact ($\lesssim$100 pc) regions.
4. These results taken together suggest that star formation in these galaxies occurs in two "extreme forms":
   (a) a relatively rare "active" mode characterized by hot dust, suppressed AFEs, high pressure, intense ultraviolet radiation field, and compact size;
   (b) a more common "passive" mode characterized by photospheric $K - L$ colors, with moderate extinction, and less extreme physical conditions.
5. The physical conditions we infer for the star-forming regions containing hot dust are similar to those created by interactions and mergers. We speculate that such intense episodes may have been more common in the past, so that the "active" regime could dominate star formation at high redshift.

Acknowledgements. The TIRGO staff was instrumental in the success of these observations. We are grateful to Giovanni Moriondo who valiantly attempted to observe for this project, and to the TIRGO Time Allocation Committee for generous time allocations. We gladly acknowledge enlightening discussions with Marc Sauvage, and would like to thank an anonymous referee for several insightful comments.

References

Abergel, A., Bernard, J. P., Boulanger, F., et al. 2002, A&A, 389, 239
Bakes, E. L. O., & Tielens, A. G. G. M. 1994, ApJ, 427, 822
Bekki, K., & Couch, W. J. 2001, ApJ, 557, L19

[8] The red $K - L$ cannot easily be attributed to nuclear activity, since LINERs tend to have NIR colors dominated by normal stellar populations (Lawrence et al. 1985).

Bessell, M. S., & Brett, J. M. 1988, PASP, 100, 1134
Boulanger, F., Reach, W. T., Abergel, A., et al. 1996, A&A, 315, L325
Calzetti, D., Meurer, G. R., Bohlin, R. C., et al. 1997, AJ, 114, 1834
Cardelli, J. A., Clayton, G. C., & Mathis, J. S. 1989, ApJ, 345, 245
Cesarsky, D., Lequeux, J., Pagani, L., et al. 1998, A&A, 337, L35
Dale, D. A., Silbermann, N. A., Helou, G., et al. 2000, AJ, 120, 583
Dale, D. A., Helou, G., Neugebauer, G., et al. 2001, AJ, 122, 1736
Elias, J. H., Frogel, J. A., Mathews, K., & Neugebauer, G. 1982, AJ, 87, 1029
Förster Schreiber, N., Roussel, N., Sauvage, M., et al. 2002, in preparation
Frogel, J. A., Persson, S. E., Aaronson, M., & Matthews, K. 1978, ApJ, 220, 75
Gallagher, J. S., & Smith, L. J. 1999, MNRAS, 304, 540
Genzel, R., Lutz, D., Sturm, E., et al. 1998, ApJ, 498, 579
Glass, I. S., & Moorwood, A. F. M. 1985, MNRAS, 214, 429
Granato, G. L., Lacey, C. G., Silva, L., et al. 2000, ApJ, 542, 710
Haas, M., Klaas, U., & Bianchi, S. 2002, A&A, 385, L23
Heckman, T. M., Armus, L., & Miley, G. K. 1990, ApJS, 74, 833
Helou, G. 1986, ApJ, 311, L33
Helou, G., Lu, N. Y., Werner, M. W., Malhotra, S., & Silbermann, N. 2000, ApJ, 532, L21
Helou, G., Ryter, C., & Soifer, B. T. 1991, ApJ, 376, 505
Hirashita, H., Hunt, L. K., & Ferrara, A. 2002, MNRAS, 330, L19
Hollenbach, D. J., & Tielens, A. G. G. 1997, ARA&A, 35, 179
Hunt, L. K., & Giovanardi, C. 1992, AJ, 104, 1018
Hunt, L. K., Hirashita, H., Thuan, T. X., Izotov, Y., & Vanzi, L. 2002, in Galaxy Evolution: Theory and observation, ed. V. Avila-Reese, C. Firmani, C. Frenk, & C. Allen, Rev. Mex. Astron. Astrofis., in press
Hunt, L. K., Mannucci, F., Testi, L., et al. 1998, AJ, 115, 2594
Hunt, L. K., Vanzi, L., & Thuan, T. X. 2001, A&A, 377, 66
Hunter, D. A., Kaufman, M., Hollenbach, D., et al. 2001, ApJ, 553, 121
Jenniskens, P., & Désert, F. X. 1993, A&A, 275, 549
Johnson, K. E., Vacca, W. D., Leitherer, C., Conti, P. S., & Lipscy, S. J. 1999, AJ, 117, 1708
Joseph, R. D., Meikle, W. P. S., Robertson, N. A., & Wright, G. S. 1984, MNRAS, 209, 111
Kaufman, M. J., Wolfire, M. G., Hollenbach, D. J., & Luhman, M. L. 1999, ApJ, 527, 795
Keto, E., Hora, J. L., Fazio, G. G., Hoffmann, W., & Deutsch, L. 1999, ApJ, 518, 183
Knapp, G. R., Gunn, J. E., & Wynn-Williams, C. G. 1992, ApJ, 399, 76
Koornneef, J. 1983, A&A, 128, 84
Lawrence, A., Ward, M., Elvis, M., et al. 1985, ApJ, 291, 117
Leitherer, C., Vacca, W. D., Conti, P. S., et al. 1996, ApJ, 465, 717
Lonsdale Persson, C. J., & Helou, G. 1987, ApJ, 314, 513
Lu, N. 1998, ApJ, 498, L65
Lutz, D., Veilleux, S., & Genzel, R. 1999, ApJ, 517, L13
Malhotra, S., Helou, G., Stacey, G., et al. 1997, ApJ, 491, L27
Malhotra, S., Hollenbach, D., Helou, G., et al. 2000, ApJ, 543, 634
Malhotra, S., Kaufman, M. J., Hollenbach, D., et al. 2001, ApJ, 561, 766
Mazzei, P., & de Zotti, G. 1994, ApJ, 427, 97
Meurer, G. R., Heckman, T. M., Leitherer, C., et al. 1995, AJ, 110, 1995
Meurer, G. R., Heckman, T. M., Lehnert, M. D., Leitherer, C., & Lowenthal, J. 1997, AJ, 114, 54
Moorwood, A. F. M., & Salinari, P. 1983, A&A, 125, 342
Moorwood, A. F. M. 1986, A&A, 166, 4
Normand, P., Rouan, D., Lacombe, F., & Tiphène, D. 1995, A&A, 297, 311
Origlia, L., Leitherer, C., Aloisi, A., Greggio, L., & Tosi, M. 2001, AJ, 122, 815
Roche, P. F., Aitken, D. K., Smith, C. H., & Ward, M. J. 1991, MNRAS, 248, 606
Sauvage, M., & Thuan, T. X. 1994, ApJ, 429, 153
Schlegel, D. J., Finkbeiner, D. P., & Davis, M. 1998, ApJ, 500, 525
Scoville, N. Z., Evans, A. S., Thompson, R., et al. 2000, AJ, 119, 991
Shioya, Y., Taniguchi, Y., & Trentham, N. 2001, MNRAS, 321, 11
Soifer, B. T., Neugebauer, G., Matthews, K., et al. 2001, AJ, 122, 1213
Somerville, R. S., Primack, J. R., & Faber, S. M. 2001, MNRAS, 320, 504
Sturm, E., Lutz, D., Tran, D., et al. 2000, A&A, 358, 481
Surace, J. A., Sanders, D. B., & Evans, A. S. 2000, ApJ, 529, 170
Thronson, H. A., & Telesco, C. M. 1986, ApJ, 311, 98
Thuan, T. X. 1983, ApJ, 268, 667
Thuan, T. X., Sauvage, M., & Madden, S. 1999, ApJ, 516, 783
Tielens, A. G. G. M., & Hollenbach, D. 1985, ApJ, 291, 722
Tran, Q. D., Lutz, D., Genzel, R., et al. 2001, ApJ, 552, 527
Turner, J. L., Beck, S. C., & Ho, P. T. P. 2000, ApJ, 532, L109
Vacca, W. D., & Conti, P. S. 1992, ApJ, 401, 543
Veilleux, S., Kim, D. C., Sanders, D. B., Mazzarella, J. M., & Soifer, B. T. 1995, ApJS, 98, 171
Watson, W. D. 1972, ApJ, 176, 103
Whitmore, B. C., Zhang, Q., Leitherer, C., et al. 1999, AJ, 118, 1551
Wilson, W. J., Schwartz, P. R., Neugebauer, G., Harvey, P. M., & Becklin, E. E. 1972, ApJ, 177, 523